

## Empty Orbitals of Adsorbates Determined by Inverse Ultraviolet Photoemission

F. J. Himpsel and Th. Fauster

*IBM T. J. Watson Research Center, Yorktown Heights, New York 10598*

(Received 1 February 1982)

The position of the lowest empty orbitals of CO and O chemisorbed on Ni(111) have been determined by use of inverse photoemission in the ultraviolet. The  $2\pi^*$  orbital of CO is lowered by 4.5 eV upon chemisorption and broadened to a 5.5-eV-wide resonance centered 3.5 eV above  $E_F$ . Chemisorbed oxygen has sharp  $2p_{x,y}$  states at 1.4 eV above  $E_F$  at  $k_{\parallel} = 0$  with the total density of states extending from  $E_F$  to  $E_F + 2$  eV in agreement with band calculations. This state disappears upon oxide formation.

PACS numbers: 73.20.Hb, 79.20.Kz

It has been recognized for a long time that the electronic states of adsorbates play an essential role in surface chemical reactions including catalysis and corrosion. Occupied states have been studied extensively by using mainly photoelectron spectroscopy. Very little is known about the empty states since the available probing techniques always create a hole when promoting an electron to an unoccupied state. This applies for optical spectroscopy, electron energy-loss spectroscopy, appearance potential spectroscopy, and partial yield photoelectron spectroscopy. The electron-hole interaction is a large perturbation to the one-electron energies in molecules. Inverse photoemission (i.e., electron in, photon out) or bremsstrahlung isochromat spectroscopy avoids this complication by putting an extra electron into an empty state without creating a hole. Recently, this technique has been extended from the x ray to the ultraviolet range<sup>1-2</sup> and has been used to probe the momentum via angle-resolved measurements.<sup>3-4</sup> Such progress opens prospects to observe electron states of adsorbates by increasing the surface sensitivity and reducing the electron-beam damage. Concurrent with experimental developments a theory of inverse photoemission has been developed<sup>5</sup> which is analogous to the theory of photoemission.

We have used inverse photoemission with a tunable photon detector in the ultraviolet to determine the energy of empty adsorbate orbitals of CO and oxygen on Ni(111). There exist many theoretical<sup>6-14</sup> and experimental<sup>15-18</sup> studies of these adsorbate systems since they are often considered as models for catalysis and corrosion, respectively. For  $\frac{1}{3}$  monolayer CO on Ni(111) we find that the  $2\pi^*$  orbital lies about 2.5 eV below the vacuum level (pulled down from about 2 eV above the vacuum level in the gas phase).<sup>19</sup> It is strongly broadened (about 5.5 eV full width at half maximum) by interaction with the continuum

of empty Ni 4s,*p* states. For  $\frac{1}{4}$  monolayer oxygen chemisorbed on Ni(111) sharp empty O  $2p$  states are found within 2 eV of the Fermi level  $E_F$ . Two layers of NiO formed by saturation exposure to oxygen exhibit a band of Ni 4s,*p* states from 2 to 4 eV above  $E_F$ .

Our experimental approach is somewhat different from previous setups<sup>1-4</sup>: We keep the incoming electron energy fixed and detect different photon energies. This corresponds to constant-final-state spectroscopy in photoemission. We have taken both angle-resolved (Fig. 1) and angle-integrated data (Figs. 2 and 3). The former are used to identify the symmetry of the orbitals; the latter to sample the density of adsorbate states. In the angle-integrated mode, electrons within a  $2\pi$  solid angle were collected by the sample and similar results are found for electron energies between 20 and 30 eV relative to the Fermi level  $E_F$  (calibrated with a gold sample). This makes sure that we sample a true density of states and rules out luminescence effects. The energy  $E$  of an empty state is determined relative to the Fermi level  $E_F$  which corresponds to the high-energy cutoff of the photon spectrum. The experiments were performed in a triple-chamber vacuum system with a working pressure in the  $10^{-11}$  Torr range. Electrons were produced by a pulse-heated tungsten filament (angle-integrated mode) and a BaO cathode (angle-resolved mode) and the emerging bremsstrahlung photons were analyzed by a Seya monochromator with a position-sensitive detector. A total energy resolution of 0.3 eV and an angular resolution of  $\lesssim 6^\circ$  were achieved in the angle-resolved mode. The work-function change  $\Delta\phi$  of the sample upon gas adsorption was determined with  $\pm 0.05$  eV accuracy from the  $I(V)$  characteristic of the cathode/sample diode. Since  $\Delta\phi$  is very sensitive to the coverage [ $\Delta\phi = +0.8$  eV (Ref. 15) for  $\frac{1}{3}$  layer CO and  $\Delta\phi = +0.5$  eV (Ref. 18) for  $\frac{1}{4}$  layer O] we could monitor surface con-

tamination and electron-beam damage effects during data taking. During measurement no detectable work-function change was found for clean Ni(111) and less than 0.2 eV work-function change for CO and O on Ni(111). The maximum electron-beam dose was  $200 \mu\text{A}/\text{cm}^2$  for 30 min at about 20 eV kinetic energy which is comparable to previous low-energy electron diffraction and Auger-electron spectroscopy studies on these systems. As a further test for electron-beam effects on CO/Ni(111) we desorbed CO thermally after data taking and obtained no remnants of cracked CO on the surface as judged by the inverse photoemission spectra and the work function.

Figure 1 shows inverse photoemission spectra for electrons incident near the sample normal ( $\theta = 0^\circ$ ) and outgoing photons with two different polarizations (*s* polarized with  $\vec{E}$  parallel to the surface and *p* polarized with  $\vec{E}$  almost perpendicular to the surface). As a result of dipole selection rules, the *s*-polarized geometry selects states of  $\Lambda_3$  symmetry ( $p_{x,y}, d_{xy}$ ). For clean Ni(111) (full curves in Fig. 1), a sharp peak is seen near  $E_F$  due to the  $\sim 0.2$ -eV-wide empty  $3d$

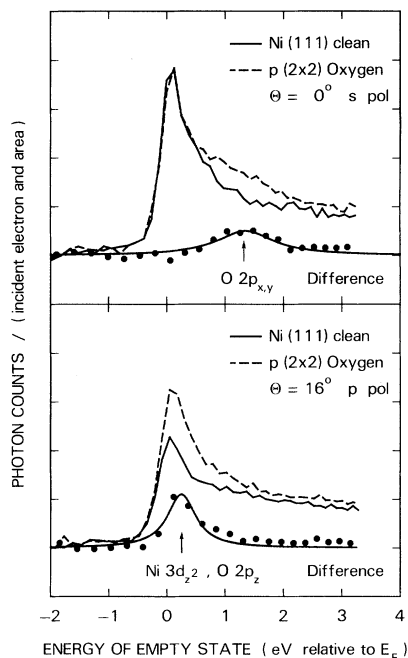


FIG. 1. Angle-resolved inverse photoemission spectra for a clean Ni(111) surface and a  $p(2 \times 2)$  overlayer of adsorbed oxygen on Ni(111). For *s*-polarized light, we find an adsorbate-induced state at  $E_F + 1.35$  eV (upper panel), whereas in *p* polarization enhanced emission is seen at  $E_F + 0.25$  eV (lower panel). The energy of the incident electrons is  $E_F + 20$  eV.

states (mostly  $d_{xy}$  character). For the Ni(111)- $p(2 \times 2)$ O structure (dashed line in Fig. 1) we find an enhancement at  $E_F + 1.35$  eV (1.2 eV wide) in *s* polarization which we assign to unoccupied oxygen  $2p_{x,y}$  states. These states are clearly separated from the Ni  $3d_{xy}$  states and lie in an absolute band gap of Ni(111) which extends from  $E_F + 0.2$  eV to  $E_F + 6$  eV at  $k_{\parallel} = 0$ . In *p* polarization, we see an enhancement at  $E_F + 0.25$  eV (0.6 eV width) which is very close to the Ni  $3d$  states but somewhat broader. This could be due to O  $2p_z$  states or to a symmetric combination of Ni  $3d$  states folded back from the Brillouin-zone boundary by the extra  $p(2 \times 2)$  lattice vector.

In order to get a picture of the total density of states, we have taken angle-integrated spectra for  $p(2 \times 2)$ O on Ni(111) [Figs. 2(b) and 3(b)]. The oxygen-induced states are centered at 0.5 eV above  $E_F$  and are substantially broader than the empty nickel *d* bands. Oxygen-induced states just above  $E_F$  have been predicted by a band calculation for a  $c(2 \times 2)$  oxygen layer on Ni(100) (Ref. 14).

Saturation oxygen exposure at room temperature is known to form two layers of NiO on Ni(111) with a reversal in the work-function change (see Ref. 18 and references therein). Ex-

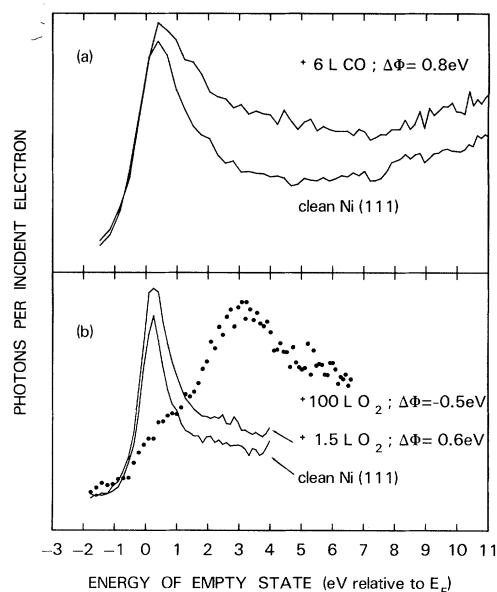


FIG. 2. Angle-integrated inverse photoemission spectra for adsorbates on Ni(111). (a)  $\frac{1}{3}$  monolayer CO/Ni(111) and clean Ni(111); (b)  $\frac{1}{4}$  monolayer chemisorbed O, clean Ni(111), and the saturation coverage of two layers, NiO (dots). The energy of the incident electrons relative to  $E_F$  was 30.5 and 22.5 eV for parts (a) and (b), respectively. (1 L =  $10^{-6}$  Torr sec.)

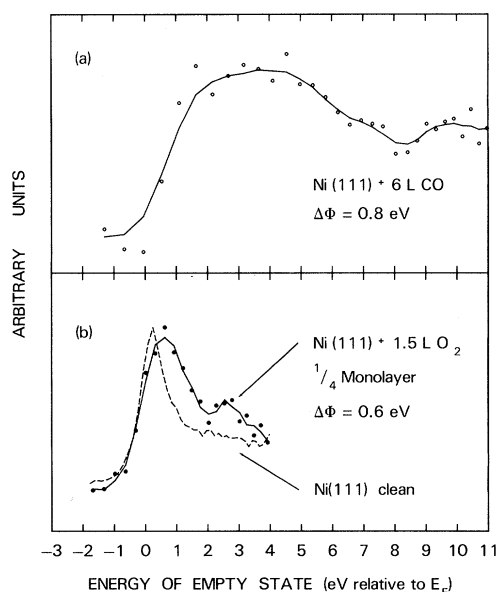


FIG. 3. Difference spectra (covered minus clean from Fig. 2) for adsorbates on Ni(111). For  $\frac{1}{3}$  monolayer CO a broad resonance is seen due to the CO  $2\pi^*$  orbital hybridized with the Ni  $4s, p$  bands. For  $\frac{1}{4}$  monolayer oxygen sharp empty O  $2p$  states exist near  $E_F$  which are distinct from the  $3d$  states of clean Ni(111) (dashed curve).

tra emission is seen for NiO between 2 and 4 eV above  $E_F$  which we assign to the Ni  $4s, p$  states according to cluster<sup>20</sup> and band<sup>21</sup> calculations. Near the Fermi level the empty states of oxidized Ni(111) are quite different from those for chemisorbed O [Fig. 2(b)] where the density of unoccupied states is enhanced by O  $2p$  states. The position of these empty O  $2p$  states seems to play an important previously unrecognized role in the energetics of surface oxidation. Little energy is needed to transfer electrons from Ni to these empty O  $2p$  states, i.e., to go from chemisorbed O to the more ionic nickel oxide. A previous inverse photoemission study of NiO has come to a similar conclusion.<sup>2</sup>

Upon CO adsorption the emission intensity increases over a wide range of photon energies, which is seen in the difference spectrum in Fig. 3(a).<sup>22</sup> From our measured work-function change  $\Delta\phi = +0.8$  eV we obtain a CO coverage of  $\frac{1}{3}$  layer which corresponds to a  $\sqrt{3} \times \sqrt{3}$  superlattice (see Ref. 15). The lowest empty orbital of CO is an antibonding  $2\pi^*$  ( $p_{x,y}$  symmetry). In the gas phase it is found as a  $\sim 2$ -eV-wide negative-ion resonance centered around 2 eV above the vacuum level,<sup>19</sup> i.e., the free CO molecule has negative electron affinity. The highest occupied orbital

( $5\sigma$ ) of free CO lies 14 eV below the vacuum level. Note that the energy to promote an electron from  $5\sigma$  to  $2\pi^*$  is about 6–9 eV (Refs. 16 and 19) which is only half as much as the difference in the energies of these orbitals. This discrepancy of up to 8 eV is due to electron-hole interaction and affects optical and energy-loss spectroscopies which involve transitions between two orbitals, whereas regular or inverse photoemission involves only one orbital. When CO is chemisorbed on a Ni surface the occupied orbitals exhibit well understood chemical and relaxation shifts.<sup>6–13</sup> The  $2\pi^*$  orbital will be lowered by an electronvolt or two because of screening by a positive image charge in the final state, but even stronger chemical effects could pull it partially below the Fermi level thus enabling “back donation” of negative charge (see Refs. 6 and 17). Cluster calculations<sup>9,10,12,13</sup> place the  $2\pi^*$  orbital of adsorbed CO at various energies between the Fermi level and the vacuum level. However, their accuracy is questionable because they place the  $2\pi^*$  orbital in free CO below the vacuum level resulting in a wrong sign for the electron affinity. Our finding of a very broad ( $\sim 5.5$  eV full width at half maximum)  $2\pi^*$  resonance for chemisorbed CO may be due to lifetime effects or mixing with the Ni bands. A better understanding of chemisorption is necessary to distinguish between these mechanisms.

We acknowledge stimulating discussions with D. Schmeisser and the help of J. J. Donelon and A. Marx. This work was supported in part by the U. S. Air Force Office of Scientific Research under Contract No. F-49620-81-C-0089.

<sup>1</sup>G. Denninger, V. Dose, and H. Scheidt, Appl. Phys. **18**, 375 (1979).

<sup>2</sup>H. Scheidt, M. Glöbl, and V. Dose, Surf. Sci. **112**, 97 (1981), and to be published.

<sup>3</sup>G. Denninger, V. Dose, and H. P. Bonzel, Phys. Rev. Lett. **48**, 279 (1982).

<sup>4</sup>D. P. Woodruff and N. V. Smith, Phys. Rev. Lett. **48**, 283 (1982).

<sup>5</sup>J. B. Pendry, Phys. Rev. Lett. **45**, 1356 (1980), and J. Phys. C **14**, 1381 (1981).

<sup>6</sup>G. Doyen and G. Ertl, Surf. Sci. **43**, 197 (1974).

<sup>7</sup>R. V. Kasowski, Phys. Rev. Lett. **37**, 219 (1976).

<sup>8</sup>K. Hermann and P. S. Bagus, Phys. Rev. B **16**, 4195 (1977).

<sup>9</sup>H. L. Yu, J. Chem. Phys. **69**, 1755 (1978).

<sup>10</sup>G. Loubriel, Phys. Rev. B **20**, 5339 (1979).

<sup>11</sup>Inder P. Batra, K. Hermann, A. M. Bradshaw, and

K. Horn, Phys. Rev. B **20**, 801 (1979).

<sup>12</sup>A. Rosén, P. Grundevik, and T. Morović, Surf. Sci. **95**, 477 (1980).

<sup>13</sup>R. P. Messmer, Surf. Sci. **106**, 225 (1981).

<sup>14</sup>A. Liebsch, Phys. Rev. B **17**, 1653 (1978).

<sup>15</sup>K. Christmann, O. Schober, and G. Ertl, J. Chem. Phys. **60**, 4719 (1974).

<sup>16</sup>G. W. Rubloff and J. L. Freeouf, Phys. Rev. B **17**, 4680 (1978).

<sup>17</sup>R. J. Smith, J. Anderson, and G. J. Lapeyre, Phys. Rev. B **22**, 632 (1980).

<sup>18</sup>A. R. Kortan and Robert L. Park, Phys. Rev. B **23**,

6340 (1981), and references therein.

<sup>19</sup>G. J. Schulz, Rev. Mod. Phys. **45**, 423 (1973).

<sup>20</sup>R. P. Messmer, C. W. Tucker, and K. H. Johnson, Surf. Sci. **42**, 341 (1974).

<sup>21</sup>T. C. Collins, A. B. Kunz, and J. L. Ivey, Int. J. Quantum Chem., Symp. **9**, 519 (1975).

<sup>22</sup>Recent angle-resolved measurements for CO on Ni(111) confirm the data shown in Figs. 2(a) and 3(a). The observed angular dependence is as expected from polarization selection rules for the  $2\pi^*$  orbital of a CO molecule bound normal to the surface [F. J. Himpsel and Th. Fauster, Phys. Rev. B **26**, 2679 (1982)].

## Atom-to-Solid Core-Level Shifts for the Lanthanides: $nl$ Dependence Introduced by Valence Changes

J. F. Herbst

*Physics Department, General Motors Research Laboratories, Warren, Michigan 48090-9055*

(Received 4 October 1982)

Free-atom-to-metal shifts of the rare-earth  $2p$ ,  $3d$ ,  $4f$ , and  $5s$  core-level binding energies have been calculated. For Pr-Sm and Tb-Tm, elements which undergo a valence change on formation of the solid, the shifts are smaller and depend significantly on the  $nl$  core-state quantum numbers. Consequently, a unique shift characterizing all core levels of a given element cannot be assumed when a configuration change involving the  $4f$  states occurs on solid formation.

PACS numbers: 71.50.+t, 79.60.Cn

Core-level binding energies determined by probes such as x-ray photoemission spectroscopy continue to provide valuable information regarding electronic structure. One focus of substantial effort is the binding-energy shift between the free-atom state and the metallic phase (see, e.g., Refs. 1-6). This paper reports the first direct calculations of such shifts for all the lanthanide elements; moreover, four different core states, the  $2p$ ,  $3d$ ,  $4f$ , and  $5s$ , are considered. The valence (or  $4f$  occupancy) change accompanying solid formation is found to produce significant quantitative differences among the shifts calculated for Pr-Sm and Tb-Tm. In particular, the

$5s$  shifts exceed those of the more spatially localized states by as much as 5 eV.

The atom-metal shift  $\delta E_B(nl)$  of a level having quantum numbers  $nl$  is here defined by

$$\delta E_B(nl) \equiv E_B^{\text{atom}}(nl) - \tilde{\Delta}_-(nl), \quad (1)$$

where  $E_B^{\text{atom}}(nl)$  and  $\tilde{\Delta}_-(nl)$  denote the free-atom and metal binding energies relative to the vacuum zero and the Fermi energy  $\epsilon_F$ , respectively. This definition is useful because binding energies are generally measured with respect to the same reference levels. Each  $E_B^{\text{atom}}(nl)$  is derived from a difference of relativistic Hartree-Fock (RHF) total energies:

$$E_B^{\text{atom}}(nl) \equiv E_{\text{ion}}^{\text{RHF}}((nl \text{ hole})4f^{k_a}(5d, 6s)^{q_a}) - E_{\text{atom}}^{\text{RHF}}(4f^{k_a}(5d, 6s)^{q_a}). \quad (2)$$

For Pr-Sm and Tb-Tm the atomic  $4f$  occupancy  $k_a$  and valence  $q_a$  differ from their metallic counterparts, as Table I indicates. Multiplet theory serves to place the  $4f$ ,  $5d$ , and  $6s$  electrons into the appropriate ground states for both initial and final configurations, while multiplet interactions between the  $nl$  hole ( $nl = 2p, 3d, 5s$ ) and the open  $4f$  and  $5d$  shells in the ionic final state are not included.

$\tilde{\Delta}_-(nl)$  is also specified by a total-energy difference:

$$\tilde{\Delta}_-(nl) \equiv E_{\text{metal}}^{\text{RHF}}((nl \text{ hole})4f^{k_m}(5d, 6s)^{q_m+1}) - E_{\text{metal}}^{\text{RHF}}(4f^{k_m}(5d, 6s)^{q_m}). \quad (3)$$